Published in final edited form as:
J Comp Neurol. 2008 September 10; 510(2): 158–174. doi:10.1002/cne.21784.

Anatomical and Neurochemical Characterization of Dopaminergic Interplexiform Processes in Mouse and Rat Retinas

PAUL WITKOVSKY[1,*], **ROBERT GÁBRIEL**[2], and **DAVID KRIŽAJ**[3]

[1] Department of Ophthalmology, New York University School of Medicine, New York, New York 10016, USA

[2] Department of Experimental Zoology and Neurobiology, University of Pecs, Pecs, H-7011, Hungary

[3] Department of Ophthalmology and Visual Sciences, Moran Eye Center, University of Utah School of Medicine, Salt Lake City, Utah 84132 USA

Abstract

Dopaminergic (DA) neurons of mouse and rat retinas are of the interplexiform subtype (DA-IPC), i.e., they send processes distally toward the outer retina, exhibiting numerous varicosities along their course. The primary question we addressed was whether distally located DA-IPC varicosities, identified by tyrosine hydroxylase (TH) immunoreactivity, had the characteristic presynaptic proteins associated with calcium-dependent vesicular release of neurotransmitter. We found that TH immunoreactive varicosities in the outer retina possessed vesicular monoamine transporter 2 and vesicular GABA transporter, but they lacked immunostaining for any of nine subtypes of voltage-dependent calcium channel. Immunoreactivity for other channels that may permit calcium influx such as certain ionotropic glutamate receptors and canonical transient receptor potential channels (TRPCs) was similarly absent, although DA-IPC varicosities did show ryanodine receptor immunoreactivity, indicating the presence of intracellular calcium stores. The synaptic vesicle proteins sv2a and sv2b and certain other proteins associated with the presynaptic membrane were absent from DA-IPC varicosities, but the vesicular SNARE protein, vamp2, was present in a fraction of those varicosities. We identified a presumed second class of IPC that is GABAergic but not dopaminergic. Outer retinal varicosities of this putative GABAergic IPC did colocalize synaptic vesicle protein 2a, suggesting they possessed a conventional vesicular release mechanism.

Indexing terms

presynaptic protein; calcium channel; immunocytochemistry; GABA; dopamine

The best-understood role of dopamine in retinal function is as a chemical messenger for light adaptation (reviewed in Witkovsky, 2004). As the natural light level rises around dawn, dopamine synthesis and release are increased. The process of diurnal light adaptation, in which cone photoreceptor-connected circuits take over from those driven by rods, involves the synchronous modulation of a very large number of cells and synapses. A central question, therefore, is how dopamine is delivered to its target sites to achieve this end. Part

[*]Correspondence to: Dr. Paul Witkovsky, Dept. Ophthalmology, New York University School of Medicine, 550 First Ave., New York, NY 10016. pw20@nyu.edu.

of the answer is that dopamine is distributed by volume conduction, i.e., it diffuses from its release sites to target receptors (Witkovsky et al., 1993) which are distributed in the retina among all major subtypes of retinal neuron and glial cell (Bjelke et al., 1996; Nguyen-Legros et al., 1999). Another factor influencing dopamine release is the intracellular distribution of release sites within the dopaminergic neurons. In some vertebrate retinas the dopaminergic neuron is an amacrine cell, but in others it an interplexiform cell (or the retina may have a mixture of the two cell types).

The term “interplexiform” was coined by Gallego (1971) to characterize a subtype of retinal amacrine cell whose processes extended into both inner and outer plexiform (synaptic) layers of the retina. This distribution of processes is not unique to amacrine interplexiform cells; all retinal bipolar neurons (Ramón y Cajal, 1892) also extend processes into both plexiform layers. However, the amacrine interplexiform neuron (IPC) is unique in having presumed output synapses in both inner and outer retinal layers.

Interplexiform neurons have been found to contain a few different neurotransmitters, including glycine (Marc, 1985; Smiley and Basinger 1988;), GABA (Nakamura et al., 1980), and dopamine (Dowling and Ehinger, 1975). In some cases there is a colocalization in the IPC of an amino acid transmitter with another neuroactive substance. For example, in an IPC of the *Xenopus* retina, glycine colocalizes with somatostatin (Smiley and Basinger, 1988) and in cat and mouse retinal IPCs GABA colocalizes with dopamine (Wässle and Chun, 1988; Contini and Raviola, 2003).

The main goals of the present study are to describe the anatomical organization of dopaminergic interplexiform (DA-IPC) processes in the outer layers of rodent (mouse and rat) retinas, and to probe whether those processes have the appropriate presynaptic machinery for vesicle-dependent release of dopamine and/or GABA. The relevance of this question is that the mechanisms by which dopamine is released are still not fully understood and appear not to be homogeneous between somatodendritic and axonal compartments of the cell. For example, in dopaminergic neurons of the substantia nigra the release of dopamine by their axonal terminals in striatum shows a more marked dependence on intracellular calcium than does release from the somatodendritic compartment (Chen et al., 2006). In mammalian retinas, dopaminergic processes have a cluster of vesicles and paramembranous membrane density typically associated with chemical synapses (Kolb et al., 1990), whereas the somatic compartment, although known to release dopamine, lacks morphologically defined presynaptic zones (Puopolo et al., 2001). Moreover, the finding that the dopaminergic IPC also is GABAergic complicates the interpretation of anatomical data in that it is still not fully established whether the presynaptic specializations of DA processes are associated with dopamine, GABA, or both (Contini and Raviola, 2003). As a further complication, on the postsynaptic side retinal dopamine receptors typically are not located immediately adjacent to the presynaptic terminal. Instead, dopamine reaches its target cells by diffusion over distances of up to tens of microns (Witkovsky et al., 1993; Bjelke et al., 1996), which means that the characteristic close apposition of pre- and postsynaptic terminal specializations may represent the GABAergic component, but not the dopaminergic component, at synapses for which the dopaminergic neuron is the presynaptic element (Contini and Raviola, 2003).

In spite of the absence of certain anatomical features associated with chemical synapses, there is substantial evidence that DA-IPCs (as well as DA amacrine cells) release dopamine by an exocytotic mechanism in the inner retina. Dopamine release, measured either from the whole retina or from individual DA perikarya, is calcium-dependent (Tamura et al., 1996; Puopolo et al., 2001). Immunocytochemical findings document the presence in DA presynaptic terminals and perikarya of the vesicular monoamine transporter type 2

(VMAT2; Puopolo et al., 2001; Witkovsky et al., 2005), which is the brain isoform responsible for transporting dopamine into synaptic vesicles or an equivalent membrane-bound compartment (Peter et al., 1995). Additional presynaptic proteins associated with vesicle docking, priming, and fusion are present in the ringlike axon terminals (Witkovsky et al., 2005), as are Ca_v 2.2 calcium channels (Witkovsky et al., 2006; also called α1B or "N" type; cf. Catterall et al., 2003, for Ca channel nomenclature) which often are implicated in transmitter release. The finding by Puopolo et al. (2001) that dopamine release from perikarya occurs as a pulsatile event indicates fusion of a dopamine-containing vesicle or similar membrane compartment, rather than by reverse transport.

The evidence for dopamine release in the outer retina, on the other hand, is not well established. In some retinas, presynaptic terminals from DA-IPCs onto horizontal and bipolar cells are reported (Dowling and Ehinger, 1975; Frederick et al., 1982; Kolb et al., 1990). The possibility, however, that the DA-IPC also colocalized another neurotransmitter was not evaluated. That is, it has not been established that the presynaptic specializations are specifically related to the release of dopamine. Given the volume conduction of dopamine in the retina (Witkovsky et al., 1993), activity-related changes in extracellular dopamine concentration cannot be readily linked to specific release sites.

The data of the present report indicate that IPC distal processes can package dopamine into membrane-bound compartments that are not conventional synaptic vesicles. In these distal processes, however, the voltage-gated calcium channels and several other presynaptic proteins that mediate calcium-dependent vesicle fusion are not observed. Our data suggest that dopamine release from DA-IPC varicosities in the outer retina may occur via an unconventional mechanism.

MATERIALS AND METHODS

Animals

C57BL/6J mice and Sprague–Dawley rats were obtained from commercial suppliers and maintained in the New York University School of Medicine (NYUSM) Animal Quarters until used. Animals were kept on a 12h:12h light:dark cycle, with lights on at 6 AM and were fed lab chow and water ad libitum.

After being transferred to the laboratory, animals were exposed to 100% CO_2 for about 30 seconds until the withdrawal response to a strong leg pinch was lost. The animal was then decapitated. Our animal handling and anesthetic procedures were approved by the NYUSM Institutional Animal Care Committee and conform to National Institutes of Health (NIH) guidelines.

Histology

Eyes were enucleated and their corneas and lenses removed. For immunocytochemistry the posterior pole of the eyecup was fixed by immersion for 1 hour at room temperature in freshly prepared 4% paraformaldehyde in 0.1 M phosphate buffer, pH 7.2, then washed 3 × 10 minutes in phosphate-buffered saline (PBS) at the same pH, before immersion in 30% sucrose (12–16 hours at 4°C). Cryostat sections were cut at 16 μm, dried for 1–2 hours at 37°C, then kept frozen until used.

For preembed electron microscopy, a modified procedure of Eldred et al. (1983) was employed. Mouse eyecups prepared as above were fixed for 1 hour in a mixture of phosphate-buffered 4% paraformaldehyde and 0.2% glutaraldehyde. Thereafter the eyecups were transferred to 4% paraformaldehyde in pH 10.4 bicarbonate buffer overnight. Following 3 × 10-minute washes in PBS, 30 minutes in 1% Na borohydride, and a further 3

× 10-minute washes in PBS, the eyecups were flash frozen on dry ice, thawed, and placed in blocking solution (PBS containing 0.1% Na azide, 0.3% Triton X-100 and 100 mg/10 mL bovine serum albumin) for 1 hour. Then the eyecups were exposed to a rabbit polyclonal anti-tyrosine hydroxylase antibody diluted 1:800 in blocking solution (primary antibodies listed in Table 1) for 16–24 hours at room temperature on a rotating table (10 rpm). Subsequently the retinas were freed from the eyecups and washed 3 × 10 minutes in PBS. Then, using the ABC kit (Vector Labs, Burlingame, CA), the antibody was biotinylated (1 hour in biotinylated antibody; 1 hour in horseradish peroxidase [HRP] complex). The subsequent diaminobenzidine reaction was monitored under a light microscope until the retina turned moderately dark (8 minutes). After a final 3 × 10 minutes in PBS the retinas were fixed in 1% OsO_4 in 0.1 M cacodylate buffer, pH 7.2. Thereafter the tissues were dehydrated in an ascending alcohol series, treated with propylene oxide, and embedded in Epon. Vertically oriented, semithin sections were obtained and immunostained DA neurons were identified. Thin sections were examined with a JEOL 1200EMX electron microscope. The diameters of round, or the long axis of irregularly shaped, cytoplasmic membrane profiles were measured in 42 varicosities showing tyrosine hydroxylase immunoreactive (TH-ir) using the NIH Image 1.55 software program (Bethesda, MD).

For fluorescence immunocytochemistry, cryostat sections were thawed, washed in PBS, then in blocking solution, before exposure to the primary antibody or a mixture of primaries for 16–20 hour at room temperature. After further washes in PBS the sections were exposed to secondary antibodies for 1–2 hours, washed again in PBS, coverslipped in Vectashield (Vector), and examined with a Nikon PM 800 confocal microscope equipped with a digital camera controlled by the Spot software program. Digital images were acquired separately from each laser channel, then recombined. Digital files were further processed with deconvolution software (AutoQuant Imaging, Watervliet, NY). Adobe Photoshop 7.0 (San Jose, CA) was used to process digital images. All images were adjusted for brightness and contrast; such adjustments were made uniformly to all parts of the image.

Antibodies

A list of the primary antibodies used and their sources is provided in Table 1. The secondary antibodies utilized were donkey antimouse Alexa 488 (Invitrogen, Carlsbad, CA) and donkey antirabbit Cy3 (Jackson Immunoresearch, West Grove, PA). No immunostaining was obtained when the primary antibody was omitted. Below we provide details of antibody production and tests of antibody specificity.

Rabbit polyclonal anti-$Ca_v1.2$ (Sigma C1603, St. Louis, MO) was raised against a synthetic peptide of amino acids 818–835 from rat brain with additional N-terminal lysine and tyrosine conjugated to keyhole limpet hemocyanin (KLH). Rabbit polyclonal anti-$Ca_v1.3$ (Sigma C1728) was raised against a synthetic peptide of amino acids 859–875 (GenBank, Bethesda, MD, accession no. P27732). Rabbit polyclonal anti-$Ca_v1.4$ was produced by Dr. J. McRory (McRory et al., 2004). The epitope was produced using the *Caulobactor* expression system (Invitrogen, Burlington, Ontario) with a synthetic peptide of amino acids 1,623–1,670 ((amino acids 1,010–1,027; accession no. AF290212); $Ca_v3.2$ (amino acids 1,195–1,273; accession no. AF290213) and $Ca_v3.3$ (amino acids 1,013–1,115; accession no. AF290214). Purified proteins were injected into rabbits and the polyclonal antibodies were immunoglobulin purified before use. Rabbit polyclonal antibodies against $Ca_v2.1$ (ACC-001), $Ca_v2.2$ (ACC-002), and $Ca_v2.3$ (ACC-006) were purchased from Alomone (Jerusalem, Israel). The $Ca_v2.1$ antibody was raised against the peptide PSSPERAPGREGPYGRE corresponding to amino acid residues 865–881 of rat $Ca_v2.1$ (accession no. P54282). The $Ca_v2.2$ antibody was raised against the peptide RH-HRHRDRDKTSASTPA corresponding to amino acid residues 851–867 of rat $Ca_v2.2$ (accession no. Q02294). The $Ca_v2.3$ antibody was raised against peptide SASQER-

SLDEGVSIDG corresponding to residues 892–907 of rat $Ca_v2.3$ (accession no. Q07652). All the anti-calcium channel antibodies were tested by Western blot on rat retinal tissue and found to stain single bands with M_r's appropriate for the alpha subunits of the Ca channel (Witkovsky et al., 2006).

The monoclonal antidopamine transporter (Chemicon, Temecula, CA; MAB 369) was raised in rat against a peptide comprised of amino acids 1–66 at the N-terminus of the human dopamine transporter fused to glutathione S-transferase. The polyclonal antidopamine transporter (Chemicon AB1591P) was raised in rabbit against a peptide consisting of amino acids 42–59 of rat brain dopamine transporter from the NH2-terminus coupled to KLH. Immunostaining was blocked by preadsorption of the primary antibody with its control peptide (Chemicon AG296).

Monoclonal antiglutamic acid decarboxylase (GAD-6; Developmental Studies Hybridoma Bank, Iowa City, IA) was raised in mouse against an affinity-purified GAD from rat brain. In a Western blot it recognized a single band of appropriate M_r. Polyclonal antirabbit GAT-1 (Chemicon AB1570) and polyclonal antirabbit GAT-3 (Chemicon AB1574) were raised against synthetic peptides of amino acids 588–599 and 607–627, respectively. Retinal immunostaining for each of these primary antibodies was blocked by preadsorption with their corresponding antigenic peptide (Johnson et al., 1996).

Rabbit polyclonal antiglutamate receptor 1 (GluR 1; Chemicon AB1504) was raised against a carboxy terminus peptide of rat GluR1 (SHSSGMPLGATGL) conjugated to BSA with glutaraldehyde. It stained a single band of appropriate M_r in Western blot analysis (manufacturer's specifications). Rabbit polyclonal anti-GluR2/-GluR3 (Chemicon AB1506) was raised against a carboxy terminus peptide (EGYNVYGIESVKI) of rat GluR2 conjugated to BSA with glutaraldehyde. It recognizes both GluR2 and GluR3 because they have nearly identical carboxy terminal sequences. Rabbit polyclonal anti-GluR4 (Chemicon AB1508) was raised against a carboxy terminus peptide (RQSSGLAVIASDLP) of rat GluR4 coupled to BSA with glutaraldehyde. In Western blots, each antiglutamate receptor antibody immunostains a single band of appropriate M_r. Moreover, all three immunostain known glutamatergic synapses in a monkey retina (Grünert et al., 2002).

The mouse monoclonal anti-IP_3 receptor (Chemicon, MAB3078) was raised against a synthetic polypeptide; KDSTEYTGPESYV coupled through a terminal cysteine to KLH). In Western blots the antibody stained a band of appropriate M_r (manufacturer's specifications)

The mouse monoclonal anti-Na channel (pan) was raised against a synthetic peptide (TEEQKKYYNAMKKLGSKK) with an N-terminal cysteine conjugated to KLH. The antigenic peptide is common to all known voltage-dependent Na channels in vertebrates. Zenisek et al. (2001) showed that goldfish retinal staining with this antibody was blocked by preadsorption with the antigenic peptide.

Polyclonal anti-ORAI1 against a portion of the calcium release-activated calcium channel was raised in rabbit against a peptide comprising amino acids 24–41 from the amino terminus of human ORAI1 (GenBank accession no. Q96D31). In Western blots against an extract of human spleen it stains a single band of M_r near 50 kD and immunostaining is blocked by preadsorption with the antigenic peptide (manufacturer's specifications).

The mouse monoclonal anti-ryanodine receptor (Affinity BioReagents, Golden, CO; MA3-925) was raised against partially purified chicken pectoral muscle ryanodine receptor. It recognizes all three isoforms of ryanodine receptor in mouse tissue. In Western blots of rat skeletal muscle extracts it detects a band at 565 kDa that corresponds to the ryanodine receptor (manufacturer's specifications).

The mouse monoclonal anti-SERCA2 ATPase (Affinity BioReagents, MA3-910) was raised against purified canine cardiac sarcoplasmic reticulum and it recognizes both SERCA2 isoforms. It immunostains a band at 110 kDa from canine skeletal muscle triads corresponding to the SERCA protein (manufacturer's specifications).

The rabbit polyclonal anti-SNAP-25 (Synaptic Systems, Germany, Cat. No. 111 002) was raised against a synthetic peptide (IDEANQRATKMLGSG) corresponding to residues 196–206 of human SNAP25, coupled to KLH by a terminal cysteine. Immunostaining was completely blocked by preadsorption of the primary antibody with its antigenic peptide (111-OP).

Rabbit polyclonal antibodies against sv2a (Synaptic Systems, Cat. No. 119 002) and sv2b (Synaptic Systems, Cat. No. 119 102) were raised against synthetic peptides (EEGFRDRAAFIRGAKD and DDYRYRDNYEGYAPND, respectively) coupled to KLH through a terminal cysteine. We found that the immunostaining of sv2a or sv2b was completely blocked (see Results) by preadsorption of the primary antibody by its antigenic peptide (119-0P and 119-1P, respectively).

The rabbit polyclonal anti-synaptotagmin 1,2 (Synaptic Systems, Cat. No. 105 002) was raised against a synthetic peptide (DDDAETGLTDGE) corresponding to residues 120–131, coupled to KLH via a terminal cysteine. This antibody was characterized by Western blots and immunocytochemistry in rodent retina by Berntson and Morgans (2003).

Mouse monoclonal anti-syntaxin1 (Sigma S0664) was raised against a synaptosomal plasma membrane fraction from adult rat hippocampus. In Western blots of mouse brain and retina this antibody stains a single, identical band near 36 kD. Retinal immunoreactivity is restricted to the inner plexiform layer (Sherry et al., 2006).

Rabbit polyclonal anti-syntaxin 3 (Synaptic Systems, 110 002) was raised against a peptide comprising amino acids 1–260 of the recombinant cytoplasmic domain of rat protein. Immunostaining was completely blocked by preadsorption of the primary antibody with the antigenic peptide (Synaptic Systems 110-3P).

Rabbit polyclonal anti-synaptobrevin (VAMP) 1 (Synaptic Systems, 104 002) was raised against a synthetic peptide (SAPAQPPAEGTEG) coupled through a terminal cysteine to KLH, corresponding to residues 2–14 of human synaptobrevin 1. Rabbit polyclonal anti-synaptobrevin 2 (Synaptic Systems, 104 202) was raised against synthetic peptide SATAATVPPAAPAGEG corresponding to residues 2–17 of rat synaptobrevin 2, and coupled to KLH through a terminal cysteine. Immunostaining to both synaptobrevin antibodies was blocked by preadsorption with their respective antigenic peptides (Synaptic Systems 104-OP and 104-2P).

Polyclonal antibodies against six members of the canonical transient receptor potential family (TRPC1, 3–7) were raised in rabbit against synthetic peptides as follows: amino acids 557–571 from human TRPC1 (Chemicon, AB5446; accession no. P48995); amino acids 822–835 from mouse TRPC3 (Chemicon AB5576; accession no. Q9QZC1); amino acids 948–958 of mouse TRPC4 (Chemicon, AB5812; accession no. Q9QUQ5); amino acids 959–973 of human TRPC5 (Chemicon, AB5849; accession no. Q9UL62); amino acids 24–38 from mouse TRPC6 (Chemicon, AB5574; accession no. Q61143); a peptide consisting of amino acids 650–700 from human TRPC7 (Chemicon, AB9326). In Western blots each anti-TRPC antibody immunostained a band of appropriate M_r (manufacturer's specifications).

Mouse monoclonal anti-TH (Chemicon, MAB 318) was raised against purified TH from PC12 cells. Rabbit polyclonal anti-TH (Chemicon, AB152) was raised against denatured TH

from rat pheochromocytoma. Either anti-TH antibody immunostains only the class of amacrine neuron also showing intrinsic dopamine fluorescence.

Mouse monoclonal anti-VGAT (Synaptic Systems, Cat. No. 131 011) was raised against synthetic peptide AEP-PVEGDIHYQR, corresponding to amino acid residues 75–87 in rat, coupled to KLH via a terminal cysteine. In Western blots the antibody immunostains a single band of appropriate M_r and this staining is blocked by preadsorption with the antigenic peptide.

Rabbit polyclonal anti-VMAT2 (PhosphoSolutions, Aurora, CO; 2200-VMAT2C) was made against the peptide SYPIGDDEESESD from the C-terminal of human VMAT2 conjugated through an N-terminal cysteine to KLH (Peter et al., 1995). It stains a single band of appropriate M_r on Western blots and does not recognize VMAT1. It colocalizes exclusively with the perikaryon and processes of retinal dopaminergic neurons (Witkovsky et al., 2005).

RESULTS

Distribution of DA-IPC processes in the outer retina

In early light microscopic studies of IPCs (Gallego, 1971; Boycott et al., 1975), one distally directed process was seen to emerge from the perikaryon and proceed vertically through the inner nuclear layer (INL) to the outer plexiform layer (OPL) where it branched and ran horizontally. This iconic image of the distal portion of an interplexiform cell does not accurately describe what is seen in mouse and rat retinas. In the description that follows the term “DA-IPC processes” will refer exclusively to those processes that are directed toward the outer retina, not the axons and dendrites of the DA-IPC neuron that are confined to the inner retina.

Since we found that DA-IPC processes in mouse and rat retinas were identical in relation to their distribution and neurochemical characteristics, we combined data from these two species into a common description. In these rodent retinas DA-IPC processes emerge not from the cell body, but rather from axons or dendrites. Using whole-mount preparations, two mouse retinas immunostained for TH were surveyed for the locus of DA-IPC process origin. In one retina, 16/289 DA-IPC processes emerged from the cell body; in the other, the comparable ratio was 15/231. Thus, only about 6% total DA-IPC processes arise from the perikaryon. This general finding is illustrated in Figure 1a–c, in which multiple DA-IPC processes are illustrated, none of which arises from a cell body.

In these same whole mounts we attempted to determine the fractions of DA-IPC processes arising either from axons or dendrites based on anatomical criteria established in an earlier study (Witkovsky et al., 2005). In the inner plexiform layer (IPL), DA axons are fine (<0.5 μm in diameter) and have a smooth profile, whereas DA dendrites are larger (1–3 μm in diameter) and have an irregular, knobby profile. Figure 1 illustrates these features and shows the origin of a DA-IPC process. In the vast majority of cases, however, it was not possible to discern the site of DA-IPC origin due to process tortuosity and the density of the DA network.

A second difference from prior descriptions of interplexiform processes is that the course taken by DA-IPC processes in rodent retinas is not necessarily vertical to the OPL (Fig. 1c). In fact, many such processes do not reach the OPL, terminating somewhere in the INL. Perhaps the most significant point is that each DA-IPC process, rather than being stout, is a slender, smooth structure, 0.1–0.2 μm in diameter but bearing multiple varicosities along its course; a process with several varicosities situated at different vertical levels of the INL is

noted (Fig. 1a) and others with multiple varicosities are shown in Figure 1c. We will assume here for the purpose of discussion that, based on their similarity in size and shape to presynaptic endings, the varicosities are the sites of dopamine release. With this in mind, the geometry of the DA-IPC processes and the distribution of their varicosities suggest that rather than being a means for bringing dopamine specifically to the OPL, they assure that dopamine is distributed more or less uniformly throughout the INL and OPL. In addition to these vertical levels, we rarely observed that DA-IPC processes extended distally beyond the OPL to end within the layer of photoreceptor cells (Fig. 1b). The data of Figure 1 emphasize that, although their density varies, DA varicosities are found at multiple horizontal levels of the neural retina.

In that regard it is instructive to look the distribution of TH-immunoreactive (ir) varicosities at different horizontal levels, as illustrated in Figure 2. In the middle panel the level of focus is at the border of INL and IPL. This is the horizontal plane in which the maximum concentration of TH-ir varicosities is seen, as well as being the location of the dopaminergic perikarya. The upper and lower panels of Figure 2 are focused on the INL, near the OPL border and on the proximal IPL, respectively. The same six dopaminergic perikarya clearly visualized in the middle panel are seen out of focus in Figure 2a,c, confirming that the same portion of the retina is being imaged. The important point is that each horizontal level has abundant DA varicosities, with a more or less even distribution within each horizontal plane.

Ultrastructure of DA-IPC varicosities

If the DA-IPC varicosities are the sites of dopamine release, and possibly also of GABA release (see below), their examination by electron microscopy (EM) might reveal presynaptic features. We treated retinas for TH-ir, then prepared them for EM (see Materials and Methods). Large perikarya and processes showing TH-ir were identified in semithin sections (Fig. 3a). Thin, vertically oriented processes were observed in the INL (Fig. 3b), which occasionally were seen to expand into varicosities 1.0–1.5 μm in diameter or long axis (Fig. 3c). As illustrated in Figure 3c, the cytoplasm of the varicosity is filled primarily with irregularly shaped membrane profiles, somewhat smaller than conventional 40–50 nm synaptic vesicles noted in an adjacent, non-TH-ir process (Fig. 3c, asterisk). We measured the diameter or long axis of 191 cytoplasmic profiles in 42 DA-IPC varicosities. The mean value ± SE was 38.87 ± 0.33 nm, range 28–50 nm. For comparison, we examined a population of 100 vesicles in rod photoreceptor terminals in the same preparation; the comparable values were 47.09 ± 0.11 nm, range 44–49 nm. The difference between these means is highly significant ($P < 0.01$) as assessed by a Student *t*-test. DA-IPC varicosities also contain 1–2 mitochondria. In contrast to what has been reported in goldfish (Dowling and Ehinger, 1975) and cat retinas (Kolb et al., 1990), we did not observe accumulations of agranular vesicles or membrane specializations typical of presynaptic endings in the DA-IPC varicosities we examined.

Neurochemical characterization of DA-IPC varicosities

TTX-sensitive Na channels—Two features suggested that the DA-IPC distal processes are axon-like. The first is developmental. Whereas DA neurons in rat retina appear around postnatal day 3 (P3) and their dendrites develop fully by P12, the DA axons and their terminals are not fully developed until P21 (Witkovsky et al., 2005). Distally directed DA-IPC processes similarly do not achieve their adult dimensions until the end of the third postnatal week. The second feature is the shape of the distally directed DA-IPC processes. As noted in Figure 1, they consist of smooth, thin processes, with a few varicosities distributed along the length, like beads on a string. This is very like the shape of DA axons in the IPL, as described above and illustrated in Figure 1.

A notable functional characteristic of DA neurons is that they have a self-generated rhythm of spiking (Gustincich et al., 1997), and they possess TTX-sensitive Na channels (Witkovsky et al., 2004). Accordingly, we used immunocytochemistry to test for the presence of such Na channels in IPC distal processes. The results are illustrated in Figure 4. It is striking that Na channel-ir is clearly seen in the DA-IPC perikarya and processes within the IPL and is just as clearly absent in the IPC distal processes.

This negative finding does not mean that the IPC distal processes will not experience a strong depolarization when a spike passes through the proximal portions of the cell. In the simplest modeling of passive signals, an unbranched process, 0.1 μm in radius, is estimated to have a length constant of ≈500 μm for passive signal spread, assuming a cytoplasmic resistance of 100 Ω cm and a membrane resistance of 5000 Ω cm^2. A more sophisticated model developed by Ellias and Stevens (1980) takes into account the current sink properties of varicosities distributed along the dendrites of amacrine cells. They assumed a process diameter of 0.1 μm, a varicosity diameter of 1.5 μm, and a frequency of 1 varicosity each 9 μm of process length, dimensions that closely approximate those of DA-IPC processes. In their simulation a conductance change that elicited an estimated 82 mV depolarization at one end of the process fell to about 50 mV over a distance of 40 μm, corresponding to the width of the INL. Their model thus suggests that even in the absence of Na channels, IPC distal processes would experience depolarizations of 10s of mV's when a spike passed through the DA cell.

VMAT2—The presence of VMAT2 indicates a capability to concentrate dopamine against a gradient into a membrane-bound compartment. VMAT2-ir has been colocalized to mouse retinal DA perikarya (Puopolo et al., 2001) and to rat retinal DA axonal terminals (Witkovsky et al., 2005). In the present investigation we found that VMAT2-ir colocalizes with DA-IPC processes (Fig. 5), where it is seen in the varicosities, but not in the slender IPC process that links adjacent varicosities. This is in contrast to TH-ir, which is uniformly distributed in all parts of the DA-IPC (cf. Figs. 1a–c, 2a, 4b,c), a difference indicating that the varicosities are the sites where dopamine is packaged and lending support to the hypothesis that the varicosities are loci of dopamine release.

VGAT—The colocalization of GABA and dopamine in mammalian retinal DA neurons (Wässle and Chun, 1988; Contini and Raviola, 2003) suggests that a functionally similar transporter to VMAT2 should be present for packaging GABA. That molecule is the vesicular GABA transporter, VGAT. We first tested for the presence of VGAT-ir in cell bodies (Fig. 6a) and in DA-IPC processes immunostained for TH. In an oblique section of mouse retina (Fig. 6b), multiple TH-ir varicosities are distributed throughout the INL and OPL. Most, but not all, of these colocalize VGAT-ir, i.e., some varicosities exhibited VMAT2-ir but lacked VGAT-ir (Fig. 6c). It can be seen that the dendritic tips of GABAergic horizontal cells in the OPL also show very strong VGAT-ir (Fig. 6b). We next tested for the colocalization of VMAT2 and VGAT-ir. As illustrated in Figure 6d–f, these two proteins were sometimes colocalized in the same DA-IPC varicosities. We also noted that some varicosities expressed VGAT-ir but lacked VMAT2-ir (Fig. 6f, asterisk), a finding that suggests that two neurochemically distinct IPCs exist. This possibility was reinforced by the distribution of the respective plasma membrane transporters of dopamine and GABA, described below.

Plasma membrane transporters of dopamine and GABA—Once dopamine and GABA are released from a presynaptic site, these two molecules can be recycled back into the releasing neuron by their respective transporters situated at the plasma membrane of the cell. The dopamine plasma membrane transporter (DAT) has been identified in rat retinal DA neurons (Cheng et al., 2006). We repeated their measures on rat and mouse retinas;

identical results were obtained in both cases, as illustrated for mouse retina in Figure 7a. DAT colocalizes to DA perikarya and processes in the IPL, but we were unable to visualize DAT-ir in DA-IPC distal processes of either mouse or rat retina (not illustrated), even when the antibody concentration was increased 10-fold over what was required to see it in the DA perikarya.

The GABA plasma membrane transporter is known to exist in three isoforms (GAT1–3) whose distribution in the rat retina has been studied (Johnson et al., 1996). Using the same antibodies employed by Johnson et al. (1996), we obtained similar immunostaining patterns. Many presumed amacrine perikarya located at the border of INL and IPL showed GAT-1-ir (Fig. 8a), as did numerous processes within the IPL (Fig. 8a,b). From the standpoint of the present study the most important observation was the presence of GAT-1-ir in fine processes that extended more or less vertically through the INL, reaching the level of the OPL, and the striking corollary observation that none of these GAT-1-ir processes colocalized TH-ir. We also did not find GAT-1-ir in DA perikarya (not illustrated). Thus, as documented in Figure 8a, TH and GAT-1 immunoreactive profiles constitute separate populations within the INL, indicating, as noted above, that there is a distinct GABAergic IPC that is not dopaminergic.

Voltage-gated calcium channels—Since the pioneering studies of Katz and co-workers (reviewed in Katz, 1969), it has been understood that release of neurotransmitter through synaptic vesicle fusion with the plasma membrane is a calcium-dependent process. An earlier survey of voltage-dependent calcium channels in rat retinal DA neurons found that five subtypes colocalized with this cell (Witkovsky et al., 2006); in particular the $Ca_V2.1$(P/Q) and $Ca_V2.2$ (N) channels were associated with the ring-like axon terminals in the IPL, where VMAT2 also is concentrated.

We began by reexamining the histological preparations used by Witkovsky et al. (2006) for colocalization of Ca channels in DA-IPC varicosities. Nine subtypes of Ca channel were studied ($Ca_V1.2$–1.4, $Ca_V2.1$–2.3, and $Ca_V3.1$–3.3); none of these colocalized to the varicosities, even though immunostaining was extremely strong within the IPL and, in some cases, also in the OPL. We extended these observations to the mouse retina, employing the same anti-Ca channel antibodies used for the rat retina. The results were identical: no immunostaining for Ca channels colocalized with DA-IPC varicosities. The results for $Ca_V2.1$ and $Ca_V2.2$ channels are illustrated in Figure 9a–d. It can be observed that immunostaining for both $Ca_V2.1$ (Fig. 9a,b) and $Ca_V2.2$ Ca channel subtypes (Fig. 9c,d) is completely absent in the DA-IPC varicosities, although the $Ca_V2.2$ channel is strongly represented in TH-ir processes within the IPL (Fig. 9c) and within terminals of horizontal cells (Fig. 9d). Strings of $Ca_V2.1$-ir puncta are observed within the INL (Fig. 9a,b), indicating an association with a retinal neuron that is not dopaminergic.

Other channels contributing to transmembrane Ca flux—Since a fraction of the DA-IPC processes end at the level of the OPL, it is conceivable that they could respond to glutamate released by photoreceptors. In the outer mammalian retina, others have shown that the ionotropic glutamate receptors present are of the AMPA and KA subtypes (Haverkamp and Wässle, 2000; deVries, 2000). Some AMPA subunits are Ca-permeable, making them a potential candidate for Ca entry into DA-IPC varicosities, although presumably only those located subjacent to photoreceptor bases would experience a sufficiently high glutamate concentration to be activated. Accordingly we examined DA-IPC varicosities in the OPL for immunoreactivity to GluR1, GluR2/3, and GluR4 antibodies. The results, however, were uniformly negative (not illustrated).

Another class of transmembrane channel that permits Ca influx and has been implicated in transmitter release, among other functions, is the transient receptor potential channel

(Munsch et al., 2003; reviewed in Ambudkar et al., 2006). We tested for the possible colocalization of several members of the so-called canonical group (TRPC 1-7) with DA-IPC processes. The results, which were invariably negative, are illustrated in Figure 10, i.e., no colocalization was observed, even though every TRPC channel tested showed a distinct pattern of immunoreactivity within the retina. Additionally we tested for Orai1 protein, a component of the calcium release-activated channel (CRAC; Vig and Kinet, 2007). Again, we found no colocalization of Orai1 in DA-IPC processes (not illustrated).

Intracellular Ca stores are also involved in the transmitter release process, as has been shown at numerous synapses in brain and retina (Llano et al., 2000; Warrier et al., 2005; Suryanarayanan and Slaughter, 2006). Two receptors located on the stores themselves mediate transmitter release, the inositol trisphosphate receptor (IP_3R) and the ryanodine receptor (RyR). We tested for these two classes and found that IP_3R-ir was not discernible, whereas RyR-ir was present in the varicosities. As illustrated in Figure 11, RyR-ir colocalizes both with TH (Fig. 11a–c) and with VMAT2 (Fig. 11d). The question of how the RyR might be activated is considered below in the Discussion section.

Presynaptic proteins—Release of neurotransmitters from synaptic vesicles is a multistep process comprising vesicle docking, priming, and fusion (reviewed in Murthy and de Camilli, 2003). These sequential steps are mediated by a stereotyped set of proteins associated with synaptic vesicle and cell surface membranes, although many of the proteins exist in multiple isoforms. We did not attempt to test every known synaptic protein for its possible colocalization in DA-IPC processes. Instead we concentrated upon a subset that have a fairly universal distribution.

Among these, the synaptic vesicle proteins SV2a and SV2b are universal constituents of synaptic vesicles (Bajjalieh et al., 1993). The presence of a third isoform, SV2c, has been observed in mammalian retina, but is reported not to be present in retina DA neurons (Wang et al., 2003). Our results are illustrated in Figure 12. Figure 12a,b shows that, although SV2a and SV2b, respectively, are abundant in both plexiform layers, they are absent from DA-IPC processes. The lower-magnification views of Figure 12c–f illustrate that SV2a- and SV2b-ir are abolished after preadsorption of the primary antibody by its antigenic peptide. These data strongly suggest that DA-IPC varicosities lack conventional agranular synaptic vesicles. On the other hand, the presumptive GABA-IPC does colocalize SV2a (Fig. 12g–i), indicating that it may have a conventional presynaptic organization.

Additionally, we examined DA-IPC processes for the presence of syntaxin 1, SNAP25, synaptotagmin 1,2, and synaptobrevin 1 and 2 (VAMP 1,2). Immunoreactivity for each of these proteins except vamp2 was absent in DA-IPC varicosities (not illustrated), even though each was associated with robust immunostaining in the IPL and, in some cases, the OPL. VAMP2 was invariably present in DA perikarya (22/22 perikarya examined; Fig. 12m) but was present only in a fraction of DA-IPC varicosities (Fig. 12j–l,m). Since VAMP2 is reported to coprecipitate with syntaxin 3 (Morgans et al., 1996) we also tested for the possible presence of syntaxin 3-ir in DA-IPC processes and in DA perikarya. We found, however, that it was absent at these sites, although present elsewhere in the retina, including in the photoreceptor terminals (not illustrated), as reported earlier by Morgans et al. (1996). As a confirmation of antibody specificity, anti-VAMP2- or syntaxin3-ir was completely lost when the primary antibodies were preadsorbed with their respective antigenic peptides; the blockage by preadsorption for VAMP2 is shown in Figure 12n.

DISCUSSION

Anatomical organization of DA-IPC processes in the outer retina

The data of the present study show that in rat and mouse retinas dopaminergic amacrine cells are of the interplexiform variety, meaning that they emit processes that run toward the outer retina. Our findings are in agreement with an earlier brief report (Nguyen-Legros et al., 1982) but provide new data about the distribution within the outer retina of IPL processes and their varicosities. In both these rodent species the distally directed DA-IPC processes emerge primarily from dendrites and course irregularly through the INL, sometimes branching, and invariably giving rise to multiple varicosities that terminate throughout the INL, the OPL, and, rarely, in the layer of photoreceptor cells. Additional sets of dopamine-containing varicosities are found at multiple levels of the IPL. These data emphasize that dopamine release sites are located at multiple planes of inner and outer retina, presumably tending to establish a uniform distribution of dopamine in retinal extracellular space.

The organization of dopaminergic synapses differs in some respects from that described for synapses utilizing fast-acting amino acids as transmitters, e.g., glutamate, GABA, and glycine. The ionotropic glutamate/GABA/glycine receptors are clustered in the postsynaptic membrane, which is closely apposed to the presynaptic ending. It should be noted that a small fraction of $GABA_A$ receptors is found in extrasynaptic sites, as reported for inner retinal synapses of the rat retina by Greferath et al. (1995). In contrast, dopamine postsynaptic receptors lie at some distance from the presynaptic terminal (Bjelke et al., 1996; Nguyen-Legros et al., 1999); dopamine reaches those receptors by diffusion. Contini and Raviola (2003) found that for retinal dopaminergic/GABAergic synapses made onto type AII amacrine cells, $GABA_A$, but not dopamine D1/D2 receptors, were clustered opposite the presynaptic ending.

Second, although dopamine is known to be released from the somatodendritic compartment of midbrain neurons in the substantia nigra (Chen et al., 2006), EM examination of this compartment has failed to identify the vesicle clusters invariably associated with amino acid synapses. Instead, VMAT2 is associated with irregularly shaped profiles that appear to be derived from smooth endoplasmic reticulum (Nirenberg et al., 1996). Our EM data of DA-IPC varicosities similarly show them filled with irregular membrane profiles, somewhat smaller than the round synaptic vesicles associated with ionotropic synapses using amino acid transmitters. This raises the possibility that EM images of DA-IPC processes in the outer retina showing conventional chemical synapses (Dowling and Ehinger, 1975; Frederick et al., 1982) may reflect the organization of a colocalized transmitter such as GABA rather than that of the dopamine system per se. On the other hand, the absence of a vesicle cluster is not a proof that dopamine is not released at that site. Voltammetric measures of extracellular dopamine indicate clearly that dopamine is released from TH-ir cell bodies, both in the retina (Puopolo et al., 2001) and in the substantia nigra (Rice et al., 1997). The available evidence, moreover, indicates that release occurs by the fusion of a vesicle or vesicle-like compartment with the surface membrane, rather than by the much more slowly acting mechanism of reverse transport (Cragg and Rice, 2004).

The bearing of these findings on the database of the present study is necessarily inferential, for there is, as yet, no direct evidence that dopamine is released from the DA-IPC distal processes. The two sets of findings that 1) distal retinal neurons (photoreceptors, bipolar cells, and horizontal cells) all have dopamine receptors (reviewed in Witkovsky, 2004); and 2) that these cells lie in close proximity to distal DA-IPC processes (Kolb et al., 1990), cannot be taken as a proof that IPC processes release dopamine, given the evidence that dopamine diffuses to distant receptors (Witkovsky et al., 1993; Bjelke et al., 1996). Yet our

findings that DA-IPC varicosities contain certain pre-synaptic proteins associated with exocytosis lend support to the supposition that they are sites of dopamine release.

Neurochemical organization of DA-IPC varicosities

DA-IPC varicosities were found to contain VMAT2 and VGAT, indicating that they can package dopamine and GABA into membrane-bound compartments. On the other hand, they lacked the voltage-gated calcium channels and many of the presynaptic vesicle and membrane proteins that permit Ca-dependent vesicular fusion. It is nevertheless counterintuitive that there should be a set of dopamine processes extending into outer retina with the capability to package dopamine, and yet not release it. If we accept that fusion of dopamine-filled packets with the surface membrane is a calcium-dependent process, as noted for DA perikarya (Puopolo et al., 2001), then we need to identify a mechanism whereby the Ca concentration of the varicosity might be increased.

The only component of a Ca regulation system in the varicosity we identified was the RyR receptor. Such receptors are known to be present on retinal intracellular stores composed of membranes derived from smooth endoplasmic reticulum and are typically caused to release Ca from stores when Ca enters the cell through plasma membrane channels that flux calcium, a process termed Ca-induced Ca release (CICR; Kriz aj et al., 2004; Bardo et al., 2006). In amacrine cells, CICR amplifies Ca signals generated by Ca entry through AMPA receptors (Chavez et al., 2006), voltage-operated Ca channels (Mitra and Slaughter, 2002), and/or reverse activation of sodium/calcium exchange (Hurtado et al., 2002). CICR provides the major component of elevated $[Ca^{2+}]_i$ in depolarized amacrine dendrites (Hurtado et al., 2006) and is a major component of vesicular GABA release at amacrine synapses in the mouse retina (Chavez et al., 2006). The mechanism underlying RyR activation in DA-IPC varicosities remains to be identified.

Is it possible that we failed to observe existing Ca channels in the varicosities? Several potential factors could be at play here. One is that the antibodies used lacked specificity for the Ca channel. This is unlikely because all were tested previously by Western blots against rat retinal tissue and each stained a single band of appropriate M_r (Witkovsky et al., 2006). In addition, each anti-Ca channel antibody has a characteristic immunostaining pattern in the retina that agrees with immunocytochemical and physiological findings by other investigators (Tamura et al., 1995; Xu et al., 2003). A second possibility is that the target varicosity is too small, but this is contradicted by our identification of anti-Ca channel-ir in dopaminergic rings in the IPL (Witkovsky et al., 2006), whose dimensions are similar to those of DA-IPC varicosities, and our ability to colocalize several other antibodies, e.g., VMAT2, to the varicosities. A third possibility is that there is a very low density of Ca channels in the varicosity plasma membrane, in the extreme case just a single channel. In fact, a simple calculation shows that a single Ca channel having only a low (5pS) conductance and a 20-ms tail current following a spike could raise $[Ca^{2+}]_i$ to micromolar levels, at least transiently. This calculation assumes a round varicosity, 1 μm in diameter and 80% filled with membranes (cf. Fig. 3c), in the absence of significant (or the presence of slow) Ca buffering. At present we have no way of evaluating this latter possibility.

In addition we lack information on a mechanism for moving dopamine/GABA from an intracellular membranous compartment to the plasma membrane and its subsequent release by exocytosis. This same difficulty holds for the somatodendritic compartment of dopaminergic neurons in the substantia nigra, in which VMAT2 is found not in synaptic vesicles, but rather in membranous components of the smooth endoplasmic reticulum (Nirenberg et al., 1996). In this regard, however, we made some progress in showing that some varicosities contained synaptobrevin2, a SNARE protein associated with vesicles (Morgans et al., 1996; Murthy and de Camilli, 2003). This datum, together with the presence

of VMAT2, indicates that the varicosities possess at least some critical elements for exocytosis.

Another provocative finding was that only a fraction of DA-IPC varicosities had synaptobrevin 2, although all had VMAT2. Moreover, synaptobrevin 2 invariably was present in the DA perikarya. Whether the absence in certain varicosities is a permanent feature, or instead indicates that presynaptic machinery can be upregulated, is a topic for future study.

In summary, based on an admittedly incomplete set of findings, we hypothesize that DA-IPC varicosities release dopamine and GABA through an exocytotic mechanism. The absence of clusters of conventional vesicles resembles what is reported for DA perikarya in substantia nigra (Nirenberg et al., 1996) and retina (Puopolo et al., 2001).

GABAergic IPC in the rodent retina

Several neurochemical findings of the present report indicate the presence of a second type of IPC which is GABAergic, but not dopaminergic. The first was the presence of the plasma membrane transporter, GAT-1, in slender, beaded processes within the INL that did not colocalize TH. Second, using an antibody against the GABA synthesizing enzyme, glutamic acid decarboxylase, we obtained an immunostaining pattern that closely resembled that of GAT-1, including intense staining of the IPL, of multiple perikarya in the proximal INL, and of fine, IPC-like processes extending toward the OPL. In some cases these fine processes were seen to emerge from GAD-ir perikarya (not illustrated). Third, the GAD-ir IPC processes colocalized SV2a, whereas the TH-ir IPC processes did not. We can rule out that the GABA-ir varicosities are simply a subset of DA-IPC varicosities, because they lacked TH-ir, which is found throughout the DA neuron. Our findings are consistent with an earlier study in cat retina (Nakamura et al., 1980) in which IPC processes that lacked catecholamine fluorescence were seen to accumulate tritiated GABA. This suggests that two distinct IPCs in mouse/rat retinas can release GABA, but apparently by different mechanisms.

Acknowledgments

We thank Dr. Elio Raviola for permitting us to view unpublished data and Drs. Arlene Hirano and Nick Brecha for providing a sample of GAD-6 antibody.

Grant sponsor: Richard H. Chartrand Foundation (to P.W.); Grant sponsor: OTKA; Grant number: K 61760 (to R.G.); Grant sponsor: National Institutes of Health (NIH); Grant number: EY 13870; Grant sponsor: James S. Adams Scholar Award and an unrestricted grant from Research to Prevent Blindness to Dept. of Ophthalmology at the University of Utah (to D.K.).

LITERATURE CITED

Ambudkar IS, Bandyopadhyay BC, Liu X, Lockwich TP, Paria B, Ong HL. Functional organization of TRPC-Ca^{2+} channels and regulation of calcium microdomains. Cell Calcium 2006;40:495–504. [PubMed: 17030060]

Bajjalieh SM, Peterson K, Linial M, Scheller RH. Brain contains two forms of synaptic vesicle protein 2. Proc Natl Acad Sci U S A 1993;90:2150–2154. [PubMed: 7681585]

Bardo S, Cavazzini MG, Emptage N. The role of the endoplasmic reticulum Ca^{2+} store in the plasticity of central neurons. Trends Pharm Sci 2006;27:78–84. [PubMed: 16412523]

Berntson AK, Morgans C. Distribution of the presynaptic calcium sensors, synaptotagmin I/II and synaptotagmin III, in the goldfish and rodent retinas. J Vision 2003;3:274–280.

Bjelke B, Goldstein M, Tionner B, Andersson C, Sesack SR, Fuxe K. Dopaminergic transmission in the rat retina: evidence for volume transmission. J Chem Neuroanat 1996;12:37–50. [PubMed: 9001947]

Boycott BB, Dowling JE, Fisher SK, Kolb H, Laties AM. Interplexiform cells of the mammalian retina and their comparison with catecholamine-containing cells. Proc Roy Soc Lond 1975;191:353–368. [PubMed: 2921]

Catterall WA, Striessnig J, Snutch TP, Perez-Reyes E. International Union of Pharmacology. XL. Compendium of voltage-gated ion channels: calcium channels. Pharmacol Rev 2003;55:579–581. [PubMed: 14657414]

Chavez AE, Singer JH, Diamond JS. Fast neurotransmitter release triggered by Ca influx through AMPA-type glutamate receptors. Nature 2006;443:705–708. [PubMed: 17036006]

Chen BT, Moran KA, Avshalumov MV, Rice ME. Limited regulation of somatodendritic dopamine release by voltage-sensitive Ca^{2+} channels contrasted with strong regulation of axonal dopamine release. J Neurochem 2006;96:645–655. [PubMed: 16405515]

Cheng Z, Zhong Y-M, Yang X-L. Expression of the dopamine transporter in rat and bullfrog retinas. Neuroreport 2006;17:773–777. [PubMed: 16708013]

Contini M, Raviola E. GABAergic synapses made by a retinal dopaminergic neuron. Proc Natl Acad Sci U S A 2003;100:1358–1363. [PubMed: 12547914]

Cragg SJ, Rice ME. Dancing past the DAT at a DA synapse. Trends Neurosci 2004;27:270–277. [PubMed: 15111009]

deVries S. Bipolar cells use kainate and AMPA receptors to filter visual information into separate channels. Neuron 2000;28:847–856. [PubMed: 11163271]

Dowling JE, Ehinger B. Synaptic organization of the amine-containing interplexiform cells of the goldfish and cebus monkey retinas. Science 1975;188:270–273. [PubMed: 804181]

Eldred WD, Zucker C, Karten HJ, Yazulla S. Comparison of fixation and penetration enhancement techniques for use in ultrastructural immunocytochemistry. J Histochem Cytochem 1983;31:285–292. [PubMed: 6339606]

Ellias SA, Stevens JK. The dendritic varicosity: a mechanism for electrically isolating the dendrites of cat retinal amacrine cells? Brain Res 1980;196:365–372. [PubMed: 6249448]

Frederick JM, Rayborn ME, Laties AM, Lam DMK, Hollyfield JG. Dopaminergic neurons in the human retina. J Comp Neurol 1982;210:65–79. [PubMed: 6127354]

Gallego, A. Horizontal and amacrine cells in the mammal's retina. Visual processes in vertebrates. In: Shipley, T.; Dowling, JE., editors. Vision Res. Oxford: Pergamon Press; 1971. p. 33-50.

Greferath U, Grünert U, Fritschy JM, Stephenson A, Möhler H, Wässle H. GABAA receptor subunits have differential distributions in the rat reina: in situ hybridization and immunohistochemistry. J Comp Neurol 1995;353:553–571. [PubMed: 7759615]

Grünert U, Haverkamp S, Fletcher EL, Wässle H. Synaptic distribution of ionotropic glutamate receptors in the inner plexiform layer of the primate retina. J Comp Neurol 2002;447:138–151. [PubMed: 11977117]

Gustincich S, Feigenspan A, Wu DK, Koopman LJ, Raviola E. Control of dopamine release in the retina: a transgenic approach to neural networks. Neuron 1997;18:723–736. [PubMed: 9182798]

Haverkamp S, Wässle H. Immunocytochemical analysis of the mouse retina. J Comp Neurol 2000;424:1–23. [PubMed: 10888735]

Hurtado J, Borges S, Wilson M. Na(+)-Ca (2+) exchanger controls the gain of the Ca(2+) amplifier in the dendrites of amacrine cells. J Neurophysiol 2002;88:2765–2777. [PubMed: 12424311]

Johnson J, Chen TK, Rickman DW, Evans C, Brecha NC. Multiple g-aminobutyric acid plasma membrane transporters (GAT-1, GAT-2, GAT-3) in the rat retina. J Comp Neurol 1996;375:212–224. [PubMed: 8915826]

Katz, B. The Sherrington Lectures X. Liverpool University Press; 1969. The release of neural transmitter substances; p. 1-59.

Kolb H, Cuenca N, Wang H-H, Dekorver L. The synaptic organization of the dopaminergic amacrine cell in the cat retina. J Neurocytol 1990;19:343–366. [PubMed: 2391538]

Kriz aj D, Liu X, Copenhagen DR. Expression of calcium transporters in the retina of the tiger salamander (Ambystoma tigrinum). J Comp Neurol 2004;475:463–480. [PubMed: 15236230]

Llano I, Gonzalez J, Caputo C, Lai FA, Blayney LM, Tan YP, Marty A. Presynaptic calcium stores underlie large-amplitude miniature IPSCs and spontaneous calcium transients. Nat Neurosci 2000;3:1256–1265. [PubMed: 11100146]

Marc, RE. The role of glycine in retinal circuitry. In: Morgan, WW., editor. Retinal transmitters and modulators: models for the brain. Vol. 1. Boca Raton, FL: CRC Press; 1985. p. 119-158.

McRory JE, Hamid J, Doering CJ, Garcia E, Parker R, Hamming K, Chen L, Hildebrand M, Beedle AM, Feldcamp L, Zamponi GW, Snutch TP. The CACNAiF gene encodes an L-type calcium channel with unique biophysical properties and tissue distribution. J Neurosci 2004;24:1707–1728. [PubMed: 14973233]

Mitra P, Slaughter MM. Calcium-induced transitions between the spontaneous miniature outward and the transient outward currents in retinal amacrine cells. J Gen Physiol 2002;119:373–388. [PubMed: 11929887]

Morgans CW, Brandstätter JH, Kellerman J, Betz H, Wässle H. A SNARE complex containing syntaxin 3 is present in ribbon synapses of the retina. J Neurosci 1996;16:6713–6721. [PubMed: 8824312]

Munsch T, Freichel M, Flockerzi V, Pape H-C. Contribution of transient receptor potential channels to the control of GABA release from dendrites. Proc Natl Acad Sci U S A 2003;100:16065–16070. [PubMed: 14668438]

Murthy VN, De Camilli P. Cell biology of the presynaptic terminal. Annu Rev Neurosci 2003;26:701–728. [PubMed: 14527272]

Nakamura Y, McGuire BA, Sterling P. Interplexiform cell in cat retina: identification by uptake of γ-[^{3}H]aminobutyric acid and serial reconstruction. Proc Natl Acad Sci U S A 1980;77:658–661. [PubMed: 6928650]

Nguyen-Legros J, Berger B, Vigny A, Alvarez C. Presence of interplexiform dopaminergic neurons in the rat retina. Brain Res Bull 1982;9:379–381. [PubMed: 6129041]

Nguyen-Legros J, Versaux-Botteri C, Vernier P. Dopamine receptor localization in the mammalian retina. Mol Neurobiol 1999;19:181–204. [PubMed: 10495103]

Nirenberg MJ, Chan J, Liu Y, Edwards RH, Pickel VM. Ultrastructural localization of the vesicular monoamine transporter-2 in midbrain dopaminergic neurons: potential sites for somatodendritic storage and release of dopamine. J Neurosci 1996;16:4135–4145. [PubMed: 8753875]

Peter D, Liu Y, Sternini C, de Giorgio R, Brecha N, Edwards RH. Differential expression of two vesicular monoamine transporters. J Neurosci 1995;15:6179–6188. [PubMed: 7666200]

Puopolo M, Hochstetler SE, Gustincich S, Wightman RW, Raviola E. Extransynaptic release of dopamine in a retinal neuron: activity dependence and transmitter modulation. Neuron 2001;30:211–225. [PubMed: 11343656]

Ramóny Cajal, S. La Cellule. Vol. 9. 1892. La rétine des vertebrés; p. 119-257.English translation: Thorpe SA, Glickstein M. Springfield, IL: CC Thomas. 1972

Rice ME, Cragg SJ, Greenfield SA. Characteristics of electrically evoked somatodendritic dopamine release in substantia nigra and ventral tegmental area in vitro. J Neurophysiol 1997;77:853–873. [PubMed: 9065854]

Smiley JF, Basinger SF. Somatostatin-like immunoreactivity and glycine high-affinity uptake colocalize to an interplexiform cell of the Xenopus laevis retina. J Comp Neurol 1988;274:608–618. [PubMed: 2906071]

Suryanarayanan A, Slaughter MM. Synaptic transmission mediated by internal calcium stores in rod photoreceptors. J Neurosci 2006;26:1759–1766. [PubMed: 16467524]

Tamura N, Yokotani K, Okuma Y, Okada M, Ueno H, Osumi Y. Properties of the voltage-gated calcium channels mediating dopamine and acetylcholine release from the isolated rat retina. Brain Res 1995;676:363–370. [PubMed: 7614007]

Vig M, Kinet J-P. The long and arduous road to CRAC. Cell Calcium 2007;42:157–162. [PubMed: 17517435]

Wang MM, Janz R, Belizaire R, Frishman LJ, Sherry DM. Differential distribution and developmental expression of synaptic vesicle protein 2 isoforms in the mouse retina. J Comp Neurol 2003;460:106–122. [PubMed: 12687700]

Warrier A, Borges S, Dalcino D, Walters C, Wilson M. Calcium from internal stores triggers GABA release from retinal amacrine cells. J Neurophysiol 2005;94:4196–4208. [PubMed: 16293593]

Wässle H, Chun MH. Dopaminergic and indoleamine-accumulating amacrine cells express GABA-like immunoreactivity in the cat retina. J Neurosci 1988;8:3383–3394. [PubMed: 2902202]

Witkovsky P. Dopamine and retinal function. Doc Ophthal 2004;108:17–40.

Witkovsky P, Nicholson C, Rice ME, Bohmaker K, Meller E. Extracellular dopamine concentration in the retina of the clawed frog, Xenopus laevis. Proc Natl Acad Sci U S A 1993;90:5667–5671. [PubMed: 8516316]

Witkovsky P, Veisenberger E, Haycock JW, Akopian A, Garcia-Espana A, Meller E. Activity-dependent phosphorylation of tyrosine hydroxylase in dopaminergic neurons of the rat retina. J Neurosci 2004;24:4242–4249. [PubMed: 15115820]

Witkovsky P, Arango-Gonzalez B, Haycock JW, Kohler K. Rat retinal dopaminergic neurons: differential maturation of somatodendritic and axonal compartments. J Comp Neurol 2005;481:352–362. [PubMed: 15593337]

Witkovsky P, Shen C, McRory J. Differential distribution of voltage-gated calcium channels in dopaminergic neurons of the rat retina. J Comp Neurol 2006;497:384–396. [PubMed: 16736476]

Xu HP, Zhao JW, Yang XL. Cholinergic and dopaminergic amacrine cells differentially express calcium channel subunits in the rat retina. Neuroscience 2003;118:763–768. [PubMed: 12710983]

Zenisek D, Henry D, Studholme K, Yazulla S, Matthews G. Voltage-dependent sodium channels are expressed in nonspiking retinal bipolar neurons. J Neurosci 2001;21:4543–4550. [PubMed: 11425883]

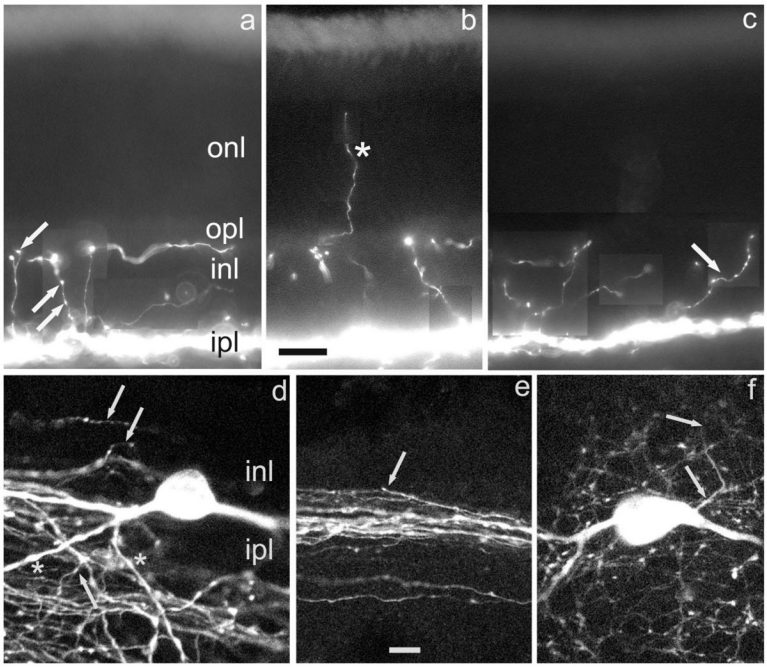

Fig. 1.

Form and location of distal DA-IPC processes. Vertical sections of mouse retina. **a–c:** Montages constructed from different focal planes. Distal DA-IPC processes are revealed by TH-ir. a: Varicosities on DA-IPC processes are indicated by arrows. b: A DA-IPC process that enters the photoreceptor layer is indicated by an asterisk. c: An obliquely oriented DA-IPC process with multiple varicosities is indicated by an arrow. DA-IPC, dopaminergic interplexiform cell; INL, inner nuclear layer; IPL, inner plexiform layer; ir, immunoreactivity; ONL, outer nuclear (photoreceptor) layer; OPL, outer plexiform layer; TH, tyrosine hydroxylase. Scale bar = 20 μm for all panels.

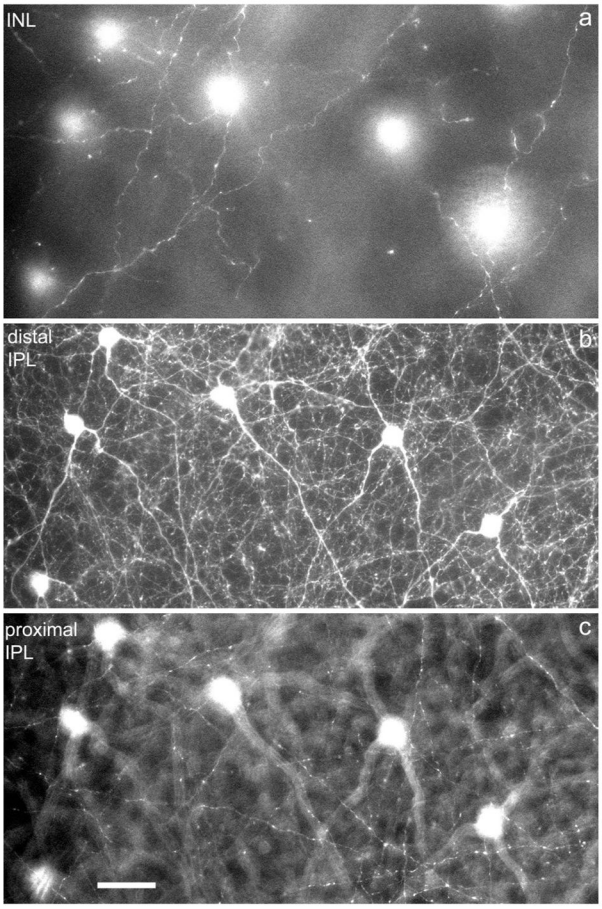

Fig. 2.

Retinal distribution of DA varicosities. **a–c:** Confocal images of the mouse retina in three horizontal planes: (a) INL close to the IPL; (b) IPL close to the INL/IPL border; (c) proximal IPL close to the layer of ganglion cells. The six DA perikarya are seen in focus in (b) and out of focus in (a) and (c). Note the presence of DA varicosities at all three levels of the retina. DA, dopaminergic.

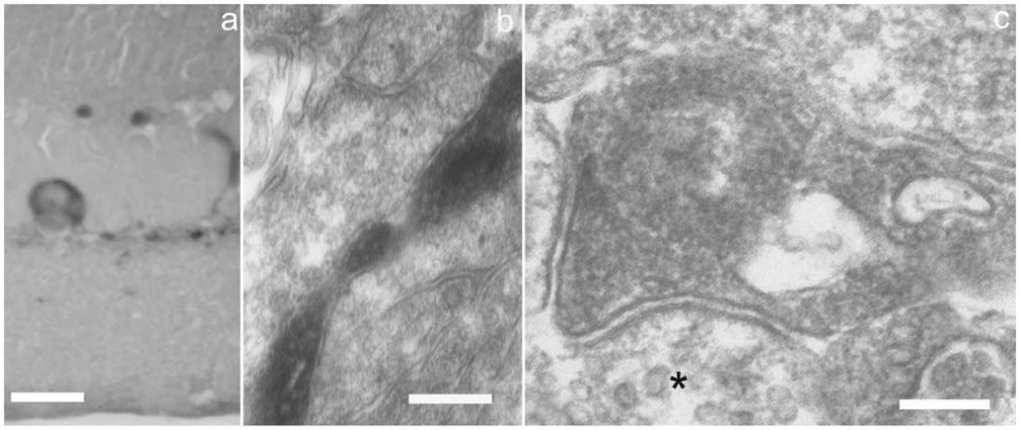

Fig. 3.

Electron microscopy of DA-IPC varicosities. **a:** Semithin vertical section of mouse retina showing a TH-ir perikaryon and processes. **b:** EM view of an ascending DA-IPC process in the INL. **c:** A DA-IPC varicosity in the distal INL showing numerous membranous compartments, usually smaller than synaptic vesicles, and two mitochondria. The asterisk in a neighboring process is adjacent to agranular synaptic vesicles of typical dimensions (40–50 nm). EM, electron microscopy. Scale bars = 20 μm in a; 250 nm in b; 150 nm in c.

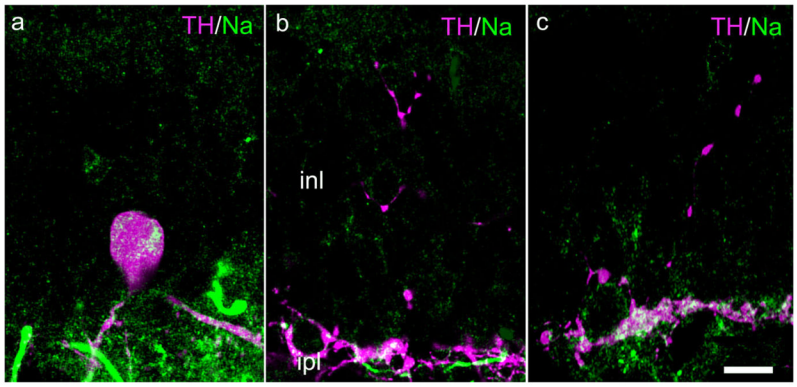

Fig. 4.

Absence of voltage-gated Na channels in DA-IPC processes. In this and subsequent color figures the colors of the label (e.g., TH/Na) correspond to the colors of the secondary antibodies, as processed in Adobe Photoshop. **a:** Vertical section of mouse retina showing TH-ir perikaryon and processes in the inner retinal with colocalized Na-ir. **b,c:** Two examples of DA-IPC TH-ir processes in the INL which lack Na-ir. Scale bar = 10 μm in c (applies to all panels).

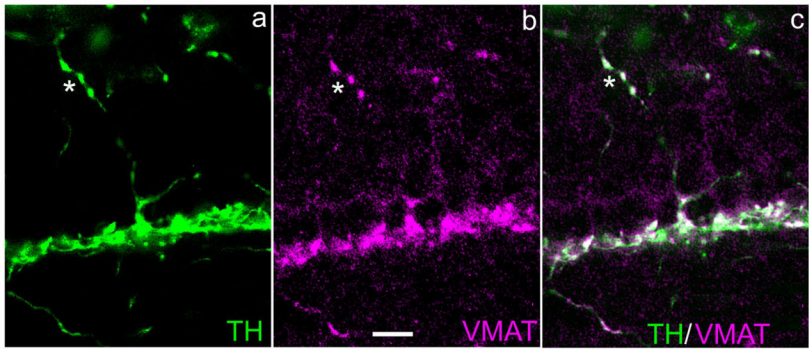

Fig. 5.

Colocalization of TH and VMAT2 in DA-IPC processes. Vertical section of mouse retina. **a,b:** TH- and VMAT2-ir in a DA-IPC process marked by an asterisk. The merged image in **(c)** shows that these two antibodies are colocalized in DA-IPC varicosities. VMAT2, vesicular monoamine transporter 2. Scale bar = 10 μm in b (applies to all panels).

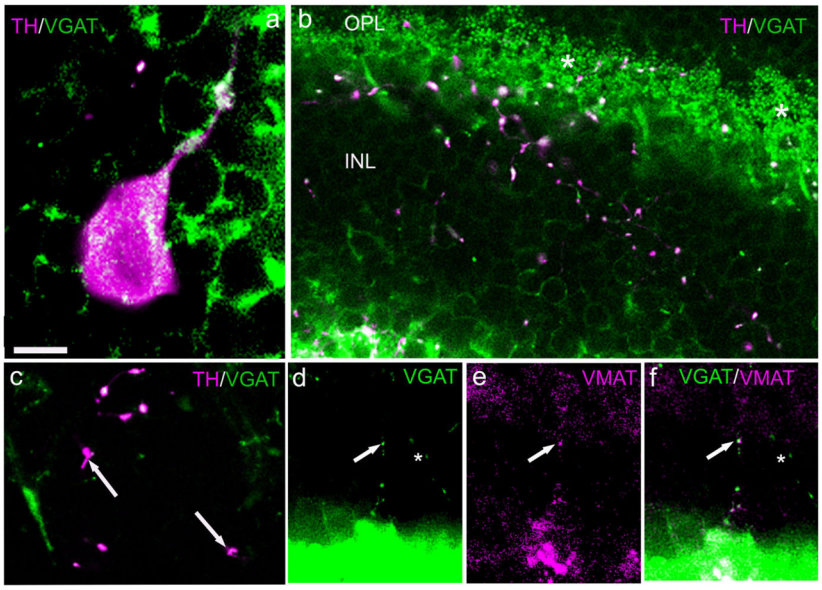

Fig. 6.

Colocalization of VGAT with TH and VMAT2 in DA-IPC processes. Rat retinal sections. **a:** Colocalization of TH- and VGAT-ir in a DA perikaryon. **b:** Oblique section extending from the IPL (lower left) to the OPL (top). In the INL and OPL multiple varicosities colocalize TH- and VGAT-ir. Asterisks indicate the intense immunostaining of horizontal terminals by VGAT. **c:** A higher-magnification view showing that some TH-ir varicosities (arrows) do not colocalize VGAT. **d–f:** Vertical sections showing, in a DA-IPC process (arrows), VGAT-ir (d), VMAT2-ir (e), and their colocalization in DA-IPC varicosities in the merged image (f). VGAT, vesicular GABA transporter. Scale bars = 10 μm in a (applies to b); 5 μm in c; 20 μm in d–f.

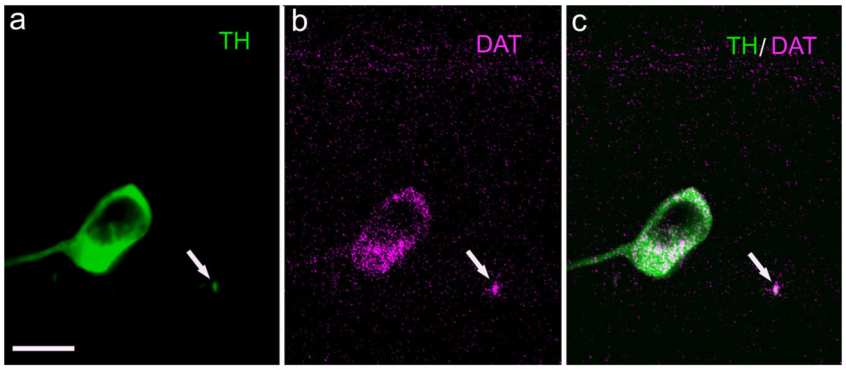

Fig. 7.

Dopamine transporter in TH-ir perikarya and processes. Vertical section of mouse retina. **a:** A TH-ir perikaryon and a profile of a TH-ir process (arrow) at the INL/IPL border. **b:** DAT-ir in these same profiles. **c:** Merged image showing colocalization of TH- and DAT-ir. DAT, dopamine transporter. Scale bar = 10 μm in a (applies to all panels).

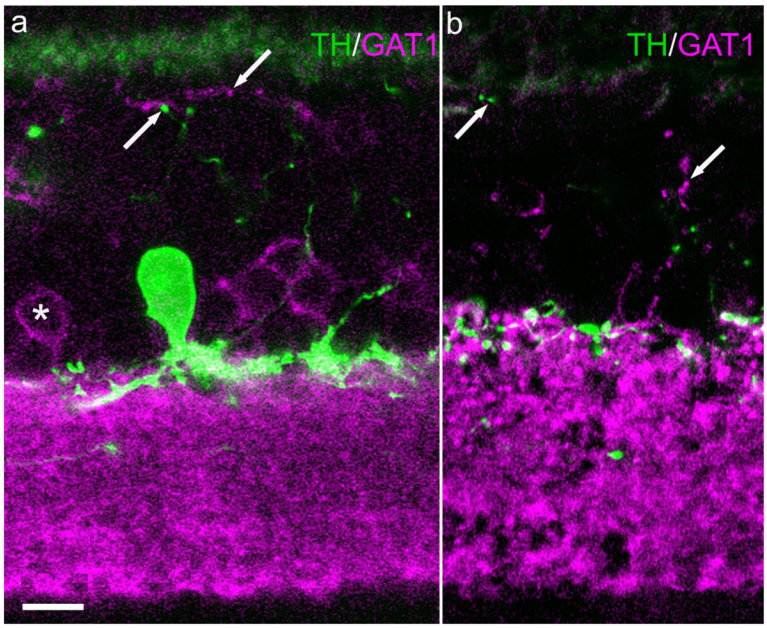

Fig. 8.

GAT-1 does not colocalize with TH in DA-IPC processes. Vertical sections mouse retina. **a:** A TH-ir perikaryon and processes are seen at the INL/IPL border. **a,b:** In the INL, TH-ir profiles (upward pointing arrow) and GAT-1-ir profiles (downward pointing arrow) constitute separate populations. This separation indicates the presence of a GABAergic IPC that is not dopaminergic. GAT-1, GABA plasma membrane transporter 1. Scale bar = 10 μm in a (applies to both panels).

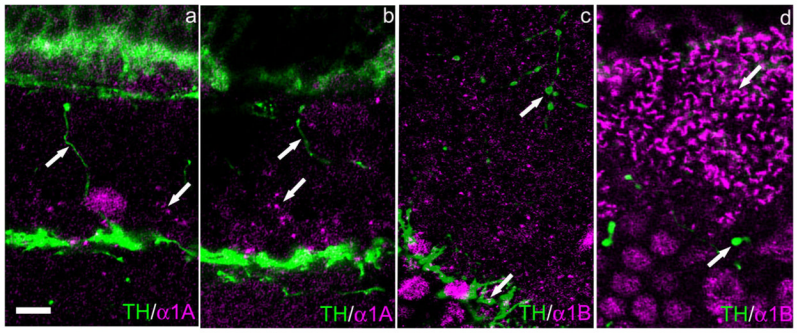

Fig. 9.

Absence of alpha1A and alpha1B Ca channels in DA-IPC varicosities. Vertical sections of mouse retina. **a,b:** TH-ir DA-IPC processes lack alpha1A-ir, although other puncta in the INL (arrow) show alpha1A-ir. **c:** TH-ir DA-IPC processes in the INL lack alpha1B-ir (upward pointing arrow), although other TH-ir processes in the IPL (downward pointing arrow) show alpha1B-ir. **d:** Horizontal cell terminals (downward pointing arrow) show strong alpha1B-ir, whereas TH-ir DA-IPC processes (upward pointing arrow) lack it. Scale bar = 10 μm in a (applies to all panels).

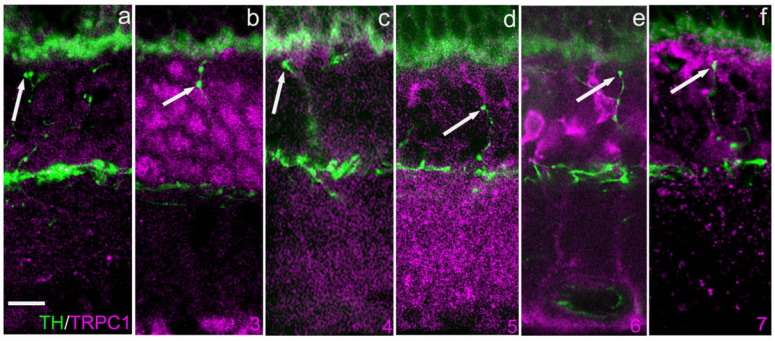

Fig. 10.

TRPC channel-ir does not colocalize with DA-IPC processes. Vertical sections of mouse retina. **a–f:** TRPC1–7-ir, respectively, in magenta. TH-ir is depicted in green. TRPC immunolabeling is diffuse and sparse for TRPC1 and TRPC4. TRPC3 immunolabeling is confined primarily to perikarya in the INL with additional puncta in the OPL. TRP5 immunolabeling is primarily in the synaptic layers (IPL and OPL). TRP6 immunolabeling is confined to the Mueller glial cells. TRP7 labeling is sparse within the IPL and OPL. Arrows point to TH-ir DA-IPC varicosities. In no case did TRPC channel-ir colocalize with TH-ir. TRPC, transient receptor potential (canonical). Scale bar = 10 μm in a (applies to all panels).

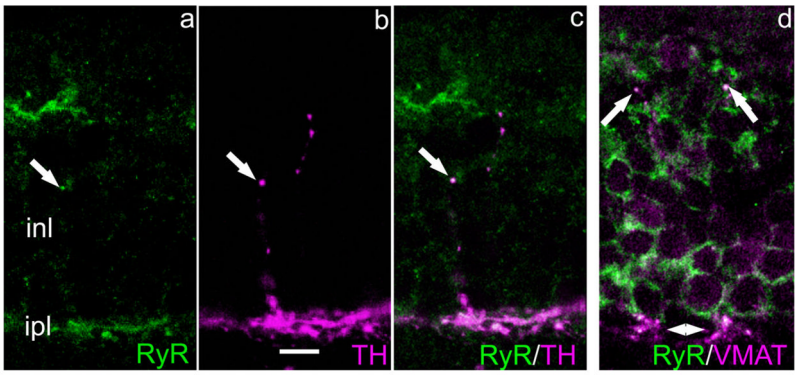

Fig. 11.

Ryanodine receptor and TH colocalize in DA-IPC processes. Vertical sections mouse retina. **a–c:** A DA-IPC varicosity shows RyR-ir (a), TH-ir (b), and the colocalization of these two antibodies in the merged image (c). In **(d)** RyR and VMAT2 colocalize in some DA-IPC varicosities (arrows). Arrowheads at the bottom of this panel indicate colocalization of RyR- and VMAT2-ir in the IPL. RyR, ryanodine receptor. Scale bar = 10 μm in b (applies to all panels).

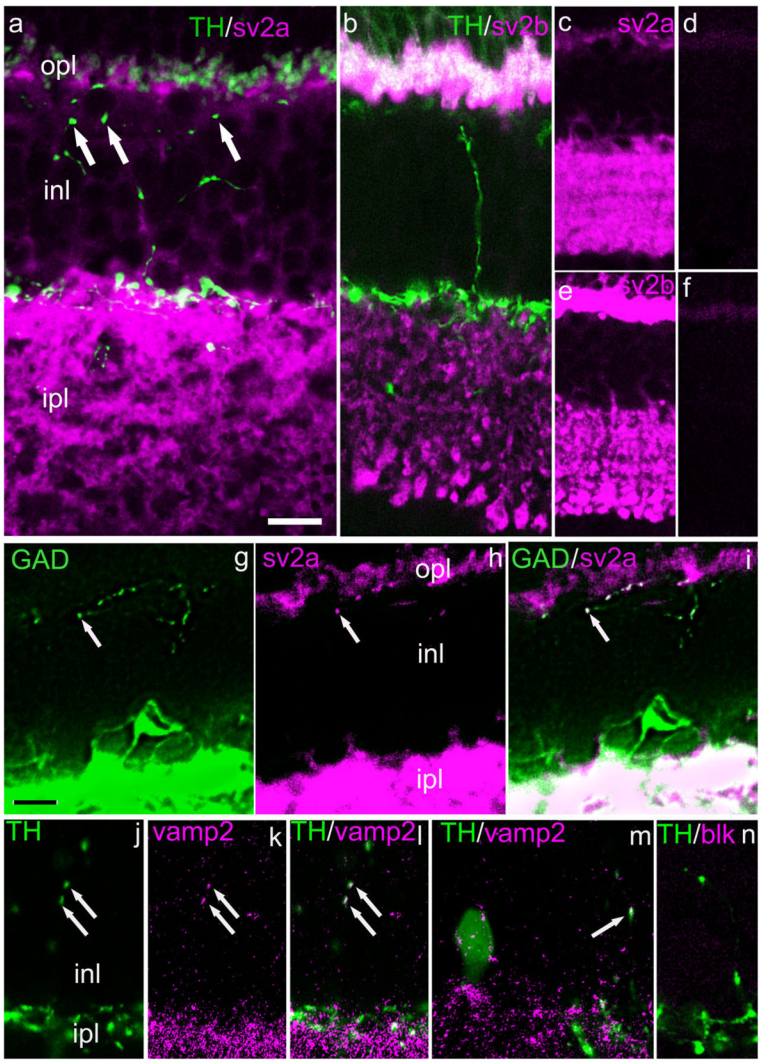

Fig. 12.

Synaptic vesicle proteins 2a and 2b in IPC processes. Vertical sections of mouse retina. **a:** Arrowheads indicate DA-IPC varicosities in the INL which lack sv2a-ir. **b:** An ascending DA-IPC process lacks sv2b-ir. **c–f:** Lower-magnification views showing retinal distribution of sv2a- (c) and sv2b-ir (d) and the loss of immunostaining following preadsorption of the antibody with its antigenic peptide (e,f). Colocalization of GAD and sv2a are shown in **(g–i)**. The arrows point to a varicosity in a GAD-ir process located adjacent to the OPL. **j–n:** Colocalization of TH and synaptobrevin (vamp)2. j–l: Two DA-IPC varicosities (arrows) show both TH-ir (j) and vamp2-ir (k). Colocalization is seen in the merged image (l). m: Both TH- and vamp2-ir are seen in a DA cell body (left) and a DA-IPC varicosity (arrow at right). n: Preadsorption of the vamp2 antibody with its antigenic peptide abolished vamp2-ir. GAD, glutamic acid decarboxylase; sv, synaptic vesicle. Scale bar = 10 μm in a for a,b; 20 μm for c–f; 10 μm in g for g–i, 12.5 μm for j–n.

J Comp Neurol. Author manuscript; available in PMC 2010 August 18.

TABLE 1

Primary Antibodies

Antibody	Manufacturer	Catalog #	Source	Poly/Mono	Effective dilution
Cav1.2	Sigma	C1603	Rabbit	P	1:500
Cav1.3	Sigma	C1728	Rabbit	P	1:200
Cav1.4	Dr. J. McRory		Rabbit	P	1:1,500
Cav2.1	Alomone	ACC-001	Rabbit	P	1:500
Cav2.2	Alomone	ACC-002	Rabbit	P	1:1,000
Cav2.3	Alomone	ACC-006	Rabbit	P	1:100
Cav3.1	Dr. J. McRory		Rabbit	P	1:1,000
Cav3.2	Dr. J. McRory		Rabbit	P	1:3,000
Cav3.3	Dr. J. McRory		Rabbit	P	1:2,000
DA Transporter	Chemicon	MAB369	Mouse	M	1:300
DA Transporter	Chemicon	AB1591P	Rabbit	P	1:400
GAD-6	U. Iowa Dev. Stud.	GAD-6-c	Mouse	M	1:1,000
GAT-1	Chemicon	AB1570	Rabbit	P	1:1,000
GAT-3	Chemicon	AB1574	Rabbit	P	1:300
GluR1	Chemicon	AB1504	Rabbit	P	1:100
GluR2/3	Chemicon	AB1506	Rabbit	P	1:200
GluR4	Chemicon	AB1508	Rabbit	P	1:200
IP3R	Chemicon	MAB3078	Mouse	M	1:200
Na channel (pan)	Sigma	S8809	Mouse	M	1:500
ORAI1	ProSci		Rabbit	P	1:50
Ryanodine receptor	Affinity Bioreagents	MA3-925	Mouse	M	1:800
SERCA2 ATPase	Affinity Bioreagents	MA3-910	Mouse	M	1:1,000
SNAP-25	Synaptic Systems	111 011	Mouse	M	1:1,000
sv2a	Synaptic Systems	119 002	Rabbit	P	1:800
sv2b	Synaptic Systems	119 102	Rabbit	P	1:200
Synaptobrevin1	Synaptic Systems	104 002	Rabbit	P	1:1,000
Synaptobrevin2	Synaptic Systems	104 202	Rabbit	P	1:1,000
Synaptotagmin 1,2	Synaptic Systems	105 002	Rabbit	P	1:1,000
Syntaxin1	Sigma	S0664	Mouse	M	1:500

Antibody	Manufacturer	Catalog #	Source	Poly/Mono	Effective dilution
Syntaxin3	Synaptic Systems	110 033	Rabbit	P	1:1,000
TRPC1	Chemicon	AB5446	Rabbit	P	1:50
TRPC3	Chemicon	AB5576	Rabbit	P	1:200
TRPC4	Chemicon	AB5812	Rabbit	P	1:50
TRPC5	Chemicon	AB5849	Rabbit	P	1:50
TRPC6	Chemicon	AB5574	Rabbit	P	1:100
TRPC7	Chemicon	AB9326	Rabbit	P	1:50
Tyrosine hydroxylase	Chemicon	MAB318	Mouse	M	1:500
Tyrosine hydroxylase	Chemicon	AB152	Rabbit	P	1:800
VGAT	Synaptic Systems	131 011	Mouse	M	1:500
VMAT2	PhosphoSolutions	2200-VMAT2C	Rabbit	P	1:3,000